Proceedings of the 17th World Congress
The International Federation of Automatic Control
Seoul, Korea, July 6-11, 2008

Centralized & Decentralized Temperature Generalized Predictive Control of a Passive-HVAC Process

R. Riadi*, R. Tawegoum*, A. Rachid, G. Chassériaux*.**

**Unité de Sciences Agronomiques Appliquées à l'Horticulture, INH-INRA-UA,
2 rue Le Nôtre 49045, Angers, France (e-mail: riad.riadi@inh.fr).
**Université de Picardie Jules Verne, IUP GEII,
33 rue Saint LEU 80000, Amiens, France (rachid@u-picardie.fr)*

Abstract: In this work, an application of conventional generalized predictive control (GPC) to a new HVAC (Heating, Ventilation, Air Conditioning) design is presented. As the process is composed of three nonlinear subsystems, two approaches for temperature control are compared; the centralized one, which solves the global control problem as a full MISO (Multi-Input Single-Output) problem, and the decentralized approach, which decomposes the global control problem into manageable subproblems. In this studied case, the system nonlinearities are seen as additive parametric uncertainties affecting the output, which appears as load disturbances to be rejected by the GPC regulator. For this purpose, both a nominal MISO discrete-time linear model of the global system and two nominal SISO discrete-time linear submodels for the principal local-systems are identified. The performances of the proposed control architectures are experimentally evaluated for a wide range of operating conditions.

1. INTRODUCTION

Nowadays agricultural exploitations have to adapt to a more competitive context and therefore to incorporate new technologies for crops growth environment, mainly climate control in growth chamber with HVAC installation (Lafont *et al.*, 2002). In general, standard HAVAC systems used in environmental control are usually composed of heating elements, a cooling system with compressor and evaporative technologies.

The studied HVAC system is a new design with innovative proprieties and environmental advantages (Tawegoum *et al.*, 2006). It does not use the more typical compression system or absorption- refrigeration cycle. It was carried out to produce a microclimate with variable temperatures and variable relative humidity setpoint values, inside the growth chambers. A complete physical model of this plant developed in (Riadi *et al.*, 2006), showed that the global system is complex and composed of three HVAC nonlinear subsystems.

Even if an adequate plant model is available, the issue of control structure selection (centralized/decentralized) needs to be addressed (Labibi *et al.*, 2003). Therefore two possible approaches are proposed in order to improve the global and the local closed loop system performance. In the first approach, named centralized MISO control strategy, the whole process is considered as full multivariable system, and all controllers contribute simultaneously in the output management. This kind of approach takes into account the coupling between subsystems, but it is usually more complicated from a design and implementation point of view.

The alternative approach consists to see the process as made of number of subsystems and to deal with the problem of controlling each of them in a mononvariable setting. Flowing this approach, decentralized SISO controllers are proposed, in the case where interaction between among subsystems is not considered and in the case where it is considered.

Generalized Predictive Control strategy is known to be an effective strategy for high performance applications, with good temporal and frequency proprieties (small overshoot, cancellation of disturbances, good stability and robustness margins) (Clarke *et al.*, 1987), (Camacho *et al.*, 1999). It allows the design of MIMO control systems that minimizes a quadratic performance index, and it can be applied to the systems involving a variable pure delay or a non-minimum phase modes. For these advantages, the GPC strategy was adopted to deal with the HVAC system difficulties.

In the second part this paper presents the plant description and in the third part, the basic points of the multivariable GPC theory leading to the elaboration of the equivalent RST controller form. After that the centralized and decentralized strategies are developed for the system. In the last part, the real time experimental results are discussed.

2. PLANT DESCRIPTION

The unit is composed of two flows: a non-saturated flow (or dry duct) and a saturated flow (or humidified duct) (Tawegoum *et al.*, 2006). As shown in "Figure 1", in the saturated air flow, fresh air is saturated in humidity after being heated by a coil resistor. Saturation operates at constant enthalpy. The saturation unit consists of a closed system, including a pump, a water tank and cross-corrugated cellulosic pads of the type using in cooling. The suction pump carries water from the tank to the top of the pads. Once a steady state of saturation is reached, the pads contain a constant mass of water with a given temperature. In the unsaturated air flow, fresh air is only heated by another resistor coil. Dry pads are included to provide pressure drop balance. The low speed of the air and of the water through the pads reduces the difference of pressure drop between the two streams.

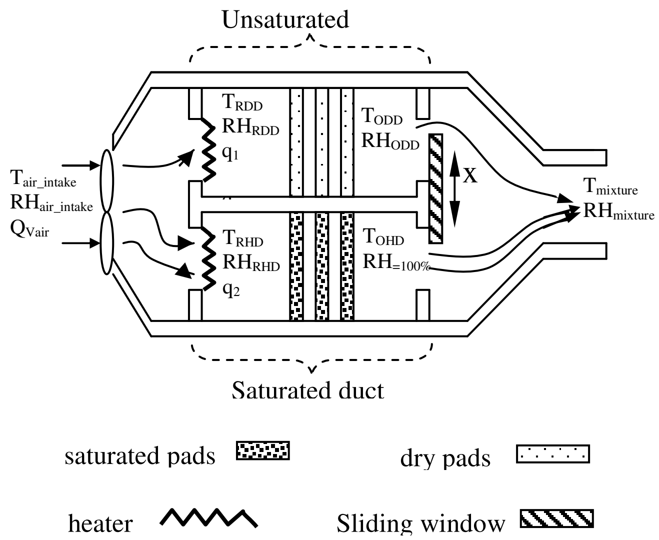

Fig. 1. Air-conditioning system

The proportional mixing of the two air flows is carried out by an aperture operated by a DC motor. Assuming that the two air flows are well mixed, a local climate can be easily produced in the growth chamber, according to the following thermodynamic equations:

$$\frac{dT_{mixture}}{dt} = -\frac{\alpha(x)\ Q_{Vair}}{V_{mixer}}\left[T_{mixture} - T_{ODD}\right] - \frac{\left(1-\alpha(x)\right)\ Q_{Vair}}{V_{mixer}}\left[T_{mixture} - T_{OHD}\right] \quad (1)$$

where $T_{mixture}$ is the air temperature (°C) in the mixer, T_{ODD} the air temperature (°C), after the dry duct, T_{OHD}, the air temperature (°C) after the humidified duct, $\alpha(x) \in [0,1]$ the volumetric air-flow percentage in the dry duct (%), x the percentage of aperture opening (%), Q_{Vair} the total volumetric air-flow rate (m^3/s), V_{mixer} the volume of the air mixer.

q_1, q_2 are the volumetric air-flow rates depending on the aperture position "Figure 1". The total volumetric air-flow rate Q_{Vair} is given as:

$$Q_{Vair} = q_1 + q_2 = \alpha(x)Q_{Vair} + (1-\alpha(x))Q_{Vair} \quad (2)$$

A complete description of the physical behaviour of the two principal ducts is given through the following steps:

1) In the dry duct, the air temperature T_{RDD} after the heater is considered to be equal to the air output temperature T_{ODD}.

The heat balance in the pads of the dry duct is given by the following equation:

$$\frac{dT_{ODD}}{dt} = \frac{-\alpha(x)Q_{V\,air}}{V_{DD}}\left[T_{ODD} - T_{air\_intake}\right] + \frac{k_{RDD}}{\rho_{air}C_{air}V_{DD}}\ U_{DD} \quad (3)$$

with T_{air_intake} the intake air temperature (°C), U_{DD} the applied voltage (V), proportional to the resistor heating in the dry duct, k_{RDD} the proportional coefficient between the voltage and the heating-power (J/sV), ρ_{air} the air density (kg/m^3), C_{air} the specific heat of air (J/kg °C), V_{DD} the volume of the dry duct (m^3).

2) In the humidified duct, the heat balance in the pads and in the heater, are respectively given by the following equations:

$$\begin{aligned}\frac{dT_{OHD}}{dt} = \frac{-(1-\alpha(x))Q_{V\,air}}{V_{pad}}\left[T_{OHD} - T_{RHD}\right] \\ - \frac{h\ A_{pad}}{\rho_{air}C_{air}V_{pad}}\left[T_{RHD} - T_{water\_intake}\right] \\ + L_V(T_{water\_intake})\frac{\rho_{water}h_{cc}A_{pad}}{\rho_{air}C_{air}V_{pad}} \\ \times\left[AH_{sat}(T_{water\_intake}) - AH_{air\_intake}\right]\end{aligned} \quad (4)$$

$$\frac{dT_{RHD}}{dt} = \frac{-(1-\alpha(x))Q_{V\,air}}{V_{RHD}}\left[T_{RHD} - T_{air\_intake}\right] + \frac{k_{RHD}}{\rho_{air}C_{air}V_{RHD}}\ U_{HD} \quad (5)$$

where T_{RHD} is the air temperature (°C) after the heater of the humidified duct, T_{water_intake} the intake water temperature in the pads of the humidified duct, U_{HD} the applied voltage (V), proportional to the heating in the humidified duct, $AH_{sat}(T_{water\_intake})$ the saturated absolute humidity at the temperature of water intake, k_{RHD} the proportional coefficient between the voltage and the heating-power (J/sV), ρ_{water} the water density (kg/m^3), C_{water} the water specific heat (J/kg °C), V_{RHD} the heater chamber volume of the humidified duct (m^3), V_{pad} the pads volume (m^3), A_{pad} the pads exchange aera (m^2), $L_V\,(T_{water\_intake})$ latent heat (J/kg of water) at the temperature of the intake water, h and h_{cc} respectively the convective heat coefficient (J/m^2s) and the mass-transfer coefficient (m^3/m^2s).

The physical models given above are complex and difficult to use for linear synthesis control objective. The air-flow measurements for the main aperture positions indicate a nonlinear relationship between the percentage of air-flow and the percentage of aperture positions (Tawegoum *et al.*, 2006).

In order to take into account these uncertainties and these complexities, the process is seen as a nominal system with additive parametric uncertainties. The predictive control algorithms based on generalized predictive control or even long range predictive control strategies have proved to be robust and efficient for industrial applications among its three freedom degrees of control parameters ($N_1, N_2,$ and λ) (Filatov *et al.*, 2004). This control strategy was applied with a different architecture in order to get better optimal performances for the global and local levels in both tracking and regulation problems.

3. MULTIVARIABLE PREDICTIVE CONTROLLER DESIGN

Without loss of generality, the multivariable GPC theory is presented here in the case of m inputs-m outputs multivariable system (Camacho *et al.*, 1999), (Boucher *et al.*, 2000).

3.1 Model definition

Similarly to the monovariable case, the following MIMO CARIMA structure is adopted for the definition of the numerical model of the system .

$$\mathbf{\Delta}_m \boldsymbol{A}\left(q^{-1}\right)\boldsymbol{y}(t) = \boldsymbol{B}\left(q^{-1}\right)\mathbf{\Delta}_m \boldsymbol{u}(t-1) + \boldsymbol{\xi}(t) \qquad (6)$$

With:

$\boldsymbol{y}(t)$: vector of the m system;

$\boldsymbol{u}(t)$: vector of the m control signals;

$\boldsymbol{\xi}(t)$: vector of uncorrelated random sequences;

$\mathbf{\Delta}_m = \Delta \boldsymbol{I}_m$, where $\boldsymbol{I}_m$ is the m order identity matrix;

$\Delta = 1 - q^{-1}$ difference operator.

$\boldsymbol{A}\left(q^{-1}\right), \boldsymbol{B}\left(q^{-1}\right)$ are polynomial matrices in the backward shift operator q^{-1}:

$$\boldsymbol{A}\left(q^{-1}\right) = \boldsymbol{I}_m + \boldsymbol{A}_1 q^{-1} + \cdots + \boldsymbol{A}_{n_a} q^{-n_a}$$
$$\boldsymbol{B}\left(q^{-1}\right) = \boldsymbol{B}_0 + \boldsymbol{B}_1 q^{-1} + \cdots + \boldsymbol{B}_{n_b} q^{-n_b}$$

3.2 Cost function

The cost function to be minimized is a weighted of squares of predicted outputs errors and control signal increments:

$$J = \sum_{i=1}^{m}\left(\sum_{j=N_{1i}}^{N_{2i}}\left(w_i(t+j) - \hat{y}_i(t+j)\right)^2 + \lambda_i \sum_{j=1}^{N_{ui}}\left(\Delta u_i(t+j-1)\right)^2\right) \qquad (7)$$

with: $\Delta u_i(t+j) = 0$ for $j \ge N_{ui}$

and $w_i(t+j)$ the setpoints at time $t+j$, $\hat{y}_i(t+j)$ the predicted outputs at time $t+j$, $\Delta u_i(t+j-1)$ the future control increments at time $t+j-1$, N_{1i}, N_{2i} the minimum and maximum prediction horizons, N_{ui}, λ_i the control prediction horizons and control weighting factors.

In our further developments, it will be considered that the prediction horizons N_{1i}, N_{2i} and N_{ui} have the same value on each channel, respectively N_1, N_2 and N_u.

3.3 Optimal predictor

Similarly to Monovariable resolution, the predictor takes polynomial matrix form:

$$\boldsymbol{y}(t+j/t) = \boldsymbol{F}_j\left(q^{-1}\right)\boldsymbol{y}(t) + \boldsymbol{H}_j\left(q^{-1}\right)\mathbf{\Delta}_m \boldsymbol{u}(t-1) + $$
$$+ \boldsymbol{G}_j\left(q^{-1}\right)\mathbf{\Delta}_m \boldsymbol{u}(t+j-1) + \boldsymbol{J}_j\left(q^{-1}\right)\boldsymbol{\xi}(t+j) \qquad (8)$$

With:

$\boldsymbol{y}(t) = \left[y_1(t)\cdots y_m(t)\right]^T$; $\boldsymbol{u}(t) = \left[u_1(t)\cdots u_m(t)\right]^T$

Where $\boldsymbol{F}_j, \boldsymbol{G}_j, \boldsymbol{H}_j, \boldsymbol{J}_j$ are $m \times m$ matrix polynomials:

$$\boldsymbol{F}_j\left(q^{-1}\right) = \sum_{i=0}^{n_a} \boldsymbol{F}_i^j q^{-i} \quad , \quad \boldsymbol{H}_j\left(q^{-1}\right) = \sum_{i=0}^{n_b-2} \boldsymbol{H}_i^j q^{-i}$$
$$\boldsymbol{G}_j\left(q^{-1}\right) = \sum_{i=0}^{n_a} \boldsymbol{G}_i^j q^{-i} \quad , \quad \boldsymbol{J}_j\left(q^{-1}\right) = \sum_{i=0}^{j-1} \boldsymbol{J}_i^j q^{-i}$$

solution of Diophantine equations:

$$\boldsymbol{J}_j\left(q^{-1}\right)\boldsymbol{A}\left(q^{-1}\right)\mathbf{\Delta}_m\left(q^{-1}\right) + q^{-j}\boldsymbol{F}_j = \boldsymbol{I}_m \qquad (9)$$
$$\boldsymbol{G}_j\left(q^{-1}\right) + q^{-(j+1)}\boldsymbol{H}_j\left(q^{-1}\right) = \boldsymbol{J}_j\left(q^{-1}\right)\boldsymbol{B}\left(q^{-1}\right) \qquad (10)$$

The optimal predictor defined between N_1 and N_2 assumes that the best prediction of the disturbance signal in the future equals zero, thus:

$$\hat{\boldsymbol{y}}(t+j/t) = \boldsymbol{F}_j\left(q^{-1}\right)\boldsymbol{y}(t) + \boldsymbol{H}_j\left(q^{-1}\right)\mathbf{\Delta}_m \boldsymbol{u}(t-1) + $$
$$+ \boldsymbol{G}_j\left(q^{-1}\right)\mathbf{\Delta}_m \boldsymbol{u}(t+j-1) \qquad (11)$$

3.4 RST polynomial controller

The minimisation of "(7)" allows obtaining the optimal controller under RST matrix form (Camcho *et al.*, 1999):

$$\boldsymbol{S}\left(q^{-1}\right)\Delta_m\left(q^{-1}\right)\boldsymbol{u}(t) = -\boldsymbol{R}\left(q^{-1}\right)\boldsymbol{y}(t) + \boldsymbol{T}\left(q^{-1}\right)\boldsymbol{w}(t) \qquad (12)$$

Where R, S, T are matrix polynomials.

4. CENTRALIZED AND DECENTRALIZED GPC APPROACHES

The behaviour of the air-conditioning system is described through the thermodynamic strategy given by the psychrometric diagram "Figure 2". The objective is to guarantee the same temperature set point for each duct (dry and humid ducts).

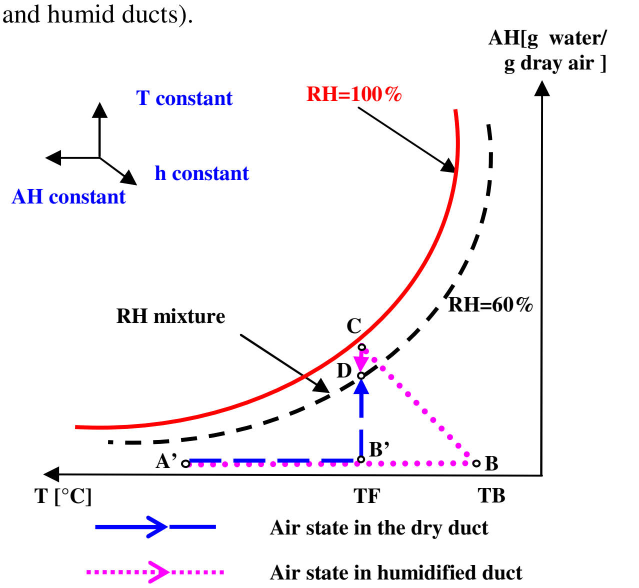

Fig. 2. Psychrometric diagram and thermodynamic strategy

4.1 Decentralised approach

Based on the conservation energy assumption, one can suppose that the same setpoint temperature will be guaranteed for the corresponding air mixture as shown in "(1)". This will be the basic idea of the decentralized control strategy by controlling independently the two different temperatures of each sub-system, in spite of air intake variation and a variable operating condition "Figure 3"

The different nominal SISO sub-systems-models are given for the 50% of aperture operating point and there structures are as following:

The dry duct temperature discrete model:

$$\left(1 + a_{11}q^{-1} + a_{12}q^{-2} + a_{13}q^{-3}\right)T_{ODD}(k) = b_{11}U_{DD}(k-1) \qquad (13)$$

The humid duct temperature discrete model:

$$\left(1 + a_{21}q^{-1} + a_{22}q^{-2} + a_{23}q^{-3}\right)T_{OHD}(k) = b_{21}U_{HD}(k-1) \qquad (14)$$

They are the model based of the decentralized GPC structure described by the "Figure 3"

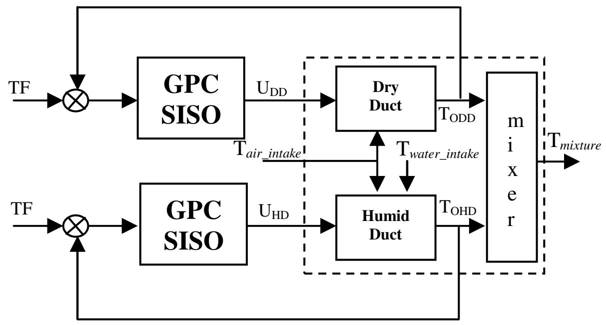

Fig. 3. Decentralized GPC structure

4.2 Centralised approach

Based on the global system point of view and on the final objectives of the mixing air temperature, the nominal full MISO system-global model is also given for the 50% of aperture operating point as flowing:

$$\begin{aligned}\left(1 + a_{11}q^{-1} + a_{12}q^{-2} + a_{13}q^{-3}\right)T_{mixture}(k) = \\ \left(b_{11}q^{-1} + b_{12}q^{-2} + b_{13}q^{-3}\right)U_{DD}(k-1) \\ +\left(b_{21}q^{-1} + b_{22}q^{-2} + b_{23}q^{-3}\right)U_{HD}(k-1) \qquad (15)\end{aligned}$$

It is the model based of the centralized GPC structure described by the "Figure 4"

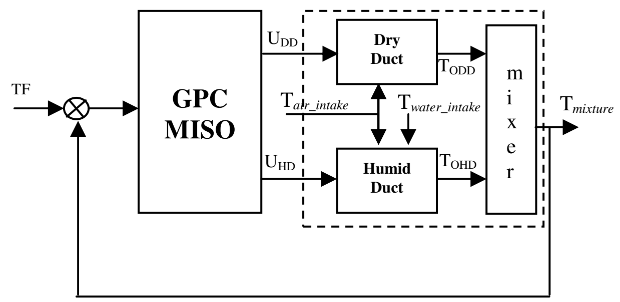

Fig. 4. Centralized GPC structure

5. EXPERIMENTAL RESULTS

The different GPC-strategies codes developed with Matlab® software were connected to the industrial automation via a local area network managed by interface developed with Delphi® software. A set of electronic units was used to apply heating voltage on the resistors or to control the DC motor and thus, the window opening rate. Measurements were carried out using Pt100 sensors for temperature and encoder sensors for position window. A sampling interval of Te=30 seconds was chosen to satisfy the predominant time constant, and data acquisition time about twelve hours. The operating point (aperture opening) values interval is $x \in [0\%, 100\%]$.

Concerning the simple decentralized approach, “Figure 6” and “Figure 7” show good local performances for different setpoint values in the two principal ducts. Both load disturbances (caused by the intake air and water temperature) and parametric disturbances (caused by the aperture commutation), are rejected. But with regard to the global performances, a static error appears in the steady state on the air mixture responses “Figure 5”. This is due to the neglected mixer temperature model part, its aero-dynamic phenomena and the non consideration of heat loss of this part of system.

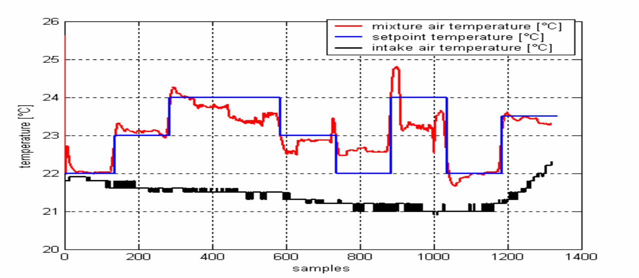

Fig. 5. Mixture air-temperature response with decentralized GPC approach

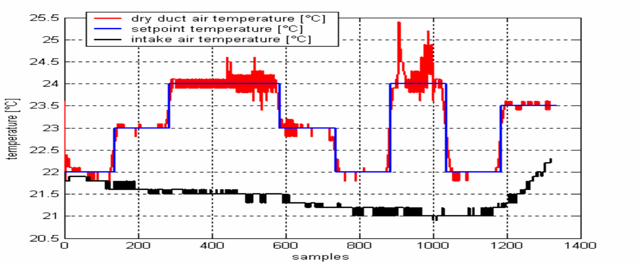

Fig. 6. Dry duct air-temperature response with decentralized GPC approach

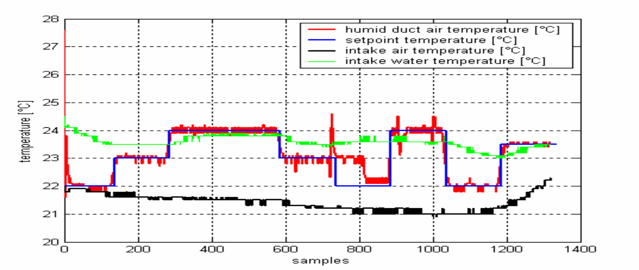

Fig. 7. Humidified duct air-temperature response with GPC decentralized approach

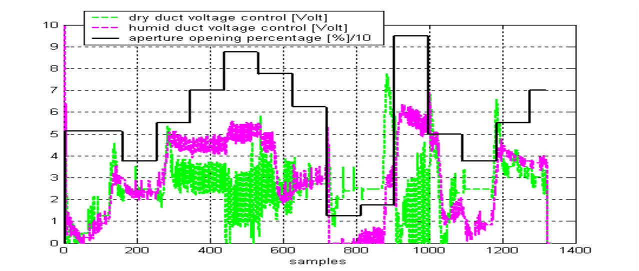

Fig. 8. Control signals and operating point variations for the decentralized GPC case

In the opposite, the centralised approach shows a good global performance represented by the air mixture temperature “Figure 9”, with accepted closed loop robustness for the both external load disturbances and parametric variation. But as negative point, the local performances, represented by the two principal ducts temperature responses, are highly decreased “Figure 10” and “Figure 11”. This is due to strategy control which doesn’t take into account the internal local performances in the minimisation criterion.

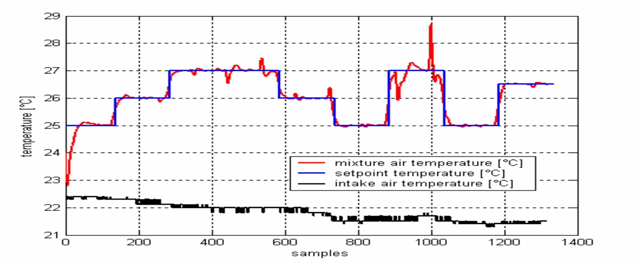

Fig. 9. Mixture air-temperature response with centralized approach

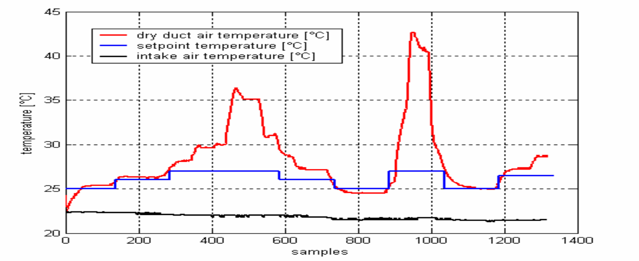

Fig. 10. Dry duct air-temperature response with centralized GPC approach

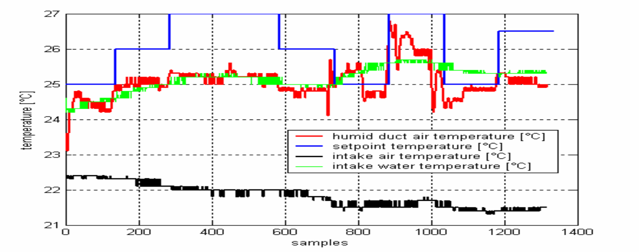

Fig. 11. Humidified duct air-temperature response with GPC centralized approach

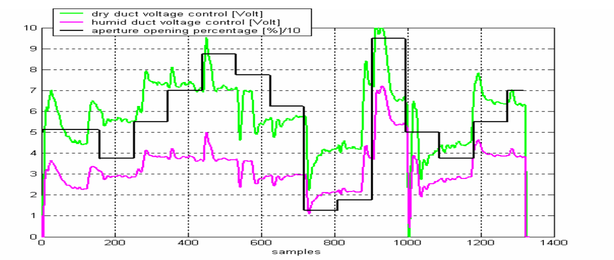

Fig. 12. Control signals and operating point variations for the centralized GPC case

In order to solve this dilemma, a solution is proposed by making a second external closed loop “Figure 13” to the decentralised as a simple supervision level, to improve the global performance in priority and to maintain the average local performance close to the setpoints. The experimental results show a good compromise with this proposed strategy to deal with this problem “Figure 14”, “Figure 15” and “Figure 16”.

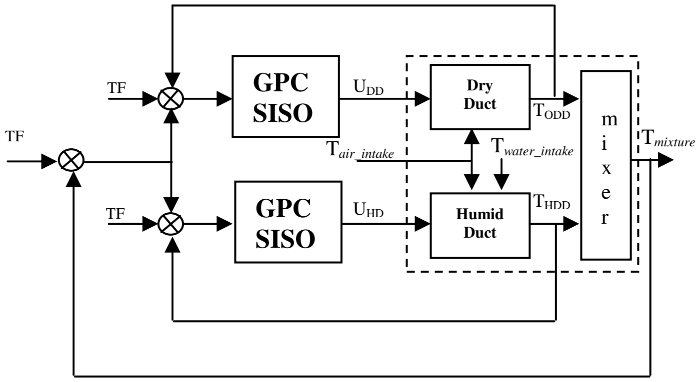

Fig. 13. Improved decentralized-GPC structure

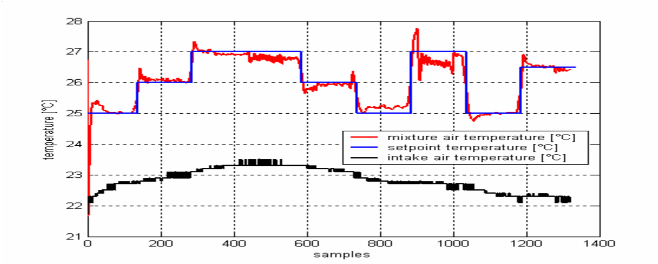

Fig. 14. Mixture air-temperature response with improved decentralized GPC approach

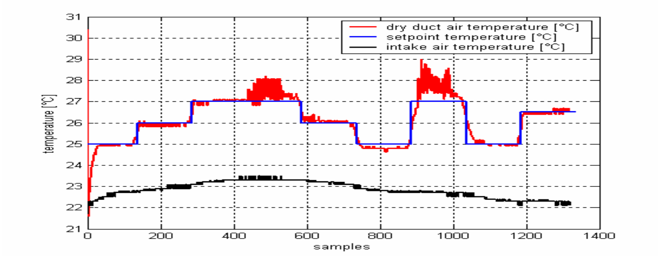

Fig. 15. Dry duct air-temperature response with improved decentralized-GPC approach

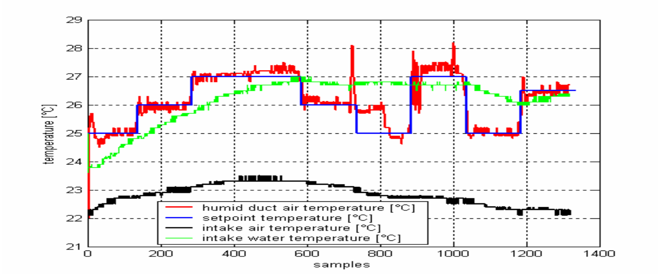

Fig. 16. Humidified duct air-temperature response with improved decentralized-GPC approach

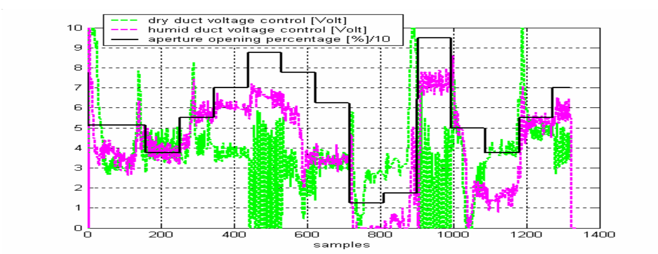

Fig. 17. Control signals and operating point variations for the improved decentralized-GPC case

6. CONCLUSIONS

This paper presents generalized predictive control with centralized and decentralized approaches, applied to the temperature control of a complex air conditioning unit. A comparative study shows the advantages and disadvantages of these strategies. The choice of the decentralized GPC architecture allowed treating the total complexity of the system control and improves the local performance, but to the detriment of global performance. Contrary to this approach, the centralized GPC architecture improves the global performance to the detriment of the local one. An incorporated external closed loop to the decentralized GPC approach, allowed guaranteeing a good compromise of local and global performances, which is wished in set-point tracking and disturbance rejection for each subsystem. Moreover, an accepted robustness is improved in spite of the parametric variation and the operating point change.

REFERENCES

Boucher, P., D. Dumur (2000).*La commande prédictive.* Méthodes et pratiques de l'ingénieur, Ed. Technip.

Camacho, E.F. and C. Bordons (1999). *Model predictive control.* Advanced textbooks in control and signal processing, Ed. Springer.

Clarke, D.W. and C. Mohtadi (1987). Generalized predictive control-part I. the basic algorithm. *Automatica,* 23(2), pp 137-148.

Dion, J.M., L. Dugard, A. Franco, M.T. Nguyen and D. Rey (1991). MIMO Predictive control Case Study: An Environmental Test Chamber. *Automatica,* Vol. 27, n. 4, pp 611-626.

Filatov, N.M. and H. Unbehauen (2004). *Adaptive dual Control: Theory and Applications.* Ed. Springer.

Labibi, B., B. Sedigh, A.K., P.J. Maralani (2003). Robust decentralized control of large-scale systems via H∞ theory and using descriptor systems representation. *International Journal of Systems Sciences,* Vol. 34, n. 1, pp 705-715.

Lafont, F. and J. F. Balmat (2002). Optimisation fuzzy control of greenhouse. *Fuzzy Stets and Systems,* Vol. 128, pp 47-59.

Riadi, R. and R. Tawegoum, A. Rachid, G. Chassériaux (2006). Modeling and Identification of Air-Conditioning Unit using the Operating Dependent Parameters Structure. *Computational Engineering in Systems Application, Beijing, China.*

Tawegoum, R. and P. E. Bournet, J. Arnould and R. Riadi (2006). Numerical investigation of an air conditioning unit to manage inside greenhouse air temperature and relative humidity. *International Symposium on Greenhouse Cooling, Almeria-Spain,* pp 115-122.